# Oxidation of stainless steel powder

Jinane Tarabay, Véronique Peres, Michèle Pijolat

"Ceramics and high-temperature composites, silicides"
CHTC9

# Oxidation of Stainless Steel Powder

**Jinane Tarabay, Véronique Peres, Michèle Pijolat**

*Ecole Nationale Supérieure des Mines, SPIN-EMSE, CNRS: LGF, F-42023 Saint-Etienne, FRANCE*

tarabay@emse.fr; peres@emse.fr; mpijolat@emse.fr

**Abstract.** To understand the corrosion behavior of a model 304L(p)-$ZrO_2$(s) composite, a 304L stainless steel powder has been studied under oxigen at high temperature. Oxidation tests were performed with thermogravimetry. The jumps method by a sudden change of the temperature was also applied to propose a kinetic model. 304L powder exhibited the same behavior than alloy plates of the same composition with a diffusion determining step, there is no influence of the oxygen partial pressure. Such a similarity was supported by SEM observations of short time and long time oxidized particles at 800 °C. Considering the first period of oxidation in the first ten hours, the external scale was mainly based of chromium oxide surrounding stainless steel particles. In this domain a mechanism is proposed and the $k_p$ value is calculated both due to the complete parabolic law and due to the areic rate of growth Φ obtained with a kinetic model specifically developed for spherical alloy particles. The values are in good agreement with the literature data.

**Keywords**: Powder, stainless steel, oxidation

## INTRODUCTION

Ceramic matrix composites dispersed with metal particles, called M(p)-CMC(s) [1], are one of the promising materials for high performance applications under some severe environment such as high temperature. This new material design offers the possibility to combine heat resistance, corrosion resistance and wear resistance due to the ceramic phase, with mechanical strength and electric conductivity provided by the metal phase.

The oxidation at 800 °C of a model M(p)-CMC(s) composite based on zirconia and 304L stainless steel materials seem to be very complicated, a rapid mass gain occurs as soon as oxygen is introduced. After this short period the mass gain curves take a parabolic shape. To understand this unusual behavior, we decide to study the oxidation of the stainless steel powder alone.

This work based on thermogravimetry (TGA) experiments under 20% $O_2$-80% He at 1 atm presents the oxidation behavior at 800°C of the stainless steel powder.

## EXPERIMENTAL PROCEDURES

The experiments were carried out on water-atomized 304 L austenitic stainless steel powder provided by Hoganas Belgium. The chemical composition of the alloy established by the supplier is summarized in Table 1. Its specific surface area measured with the BET method is 0.06 $m^2/g$. Various particle size classes, from 0-50 µm fraction up to a fraction > 100 µm, have been obtained after sieving the steel powder.

**TABLE 1. Chemical composition of 304L Stainless steel**

| Weight (%) | Fe | Cr | Ni | Si |
|---|---|---|---|---|
| | base | 18.1 | 11.3 | 0.85 |

The particle size distribution in volume, established by laser granulometry (Malvern instruments, Mastersizer 2000) reveals one main mode particle diameter at 80 µm (Figure 1).

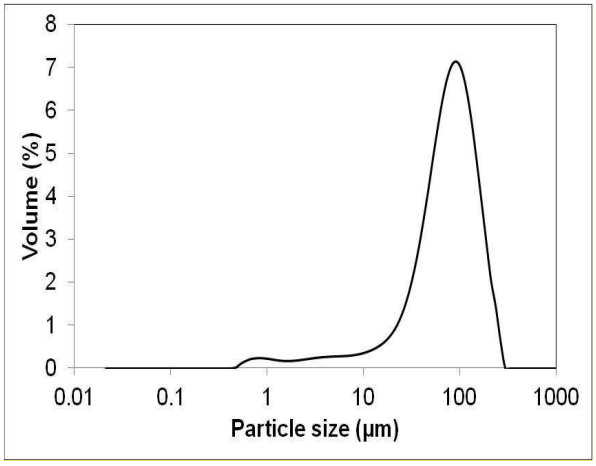


**FIGURE 1**. Grain size distribution of 304L stainless steel powder.

## Test Facility and Conditions

Oxidation experiments were performed in a symmetric thermogravimetric analyzer (SETARAM TGA16 with a thermocouple PtRh 6 % /PtRh 30 %) at 800 °C for 6 hours in a flowing mixture of helium and oxygen. The composition in oxygen was varied in the range 10 – 40 vol. %. The tests were carried out at atmospheric pressure with a total gas flow rate of 2 $L.h^{-1}$ in each furnace. Samples consist of small beds (10 mg) of stainless steel powder placed in an alumina crucible.

The TGA experiments consisted of three main consecutive steps: heating to 800 °C with a rate of 30 °C/min under helium, isothermal exposure under oxygen helium mixture at 800 °C during various periods up to 20 hours, cooling to room temperature with a rate of 30 °C/min under oxygen helium mixture. The oxygen is introduced after seven minutes at 800 °C. The oxygen impurity in helium was analyzed at the outlet of the furnace by an oxygen probe (Systech Instruments Série 900) with an accuracy of about 1 ppm at 20°C.

## RESULTS

*TGA Results*

A lack of reproducibility of the oxidation curves of 304L stainless steel powder is observed which is mainly due to a difference in particle size. The mass gain curves vs time for the as received 304L powder and for the various particles size classes are shown in Figure 2. It can be seen that a good reproducibility was obtained with each particle size class of sieved powders, whereas the curves obtained with the as received 304L powder were not so well reproducible.

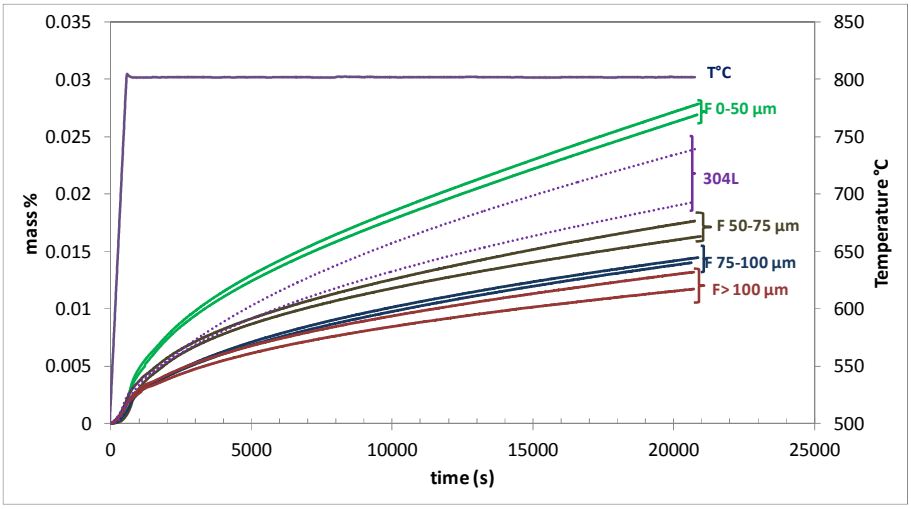


**FIGURE 2**. Mass gain (%) versus time of as received and sieved 304L stainless steel powders oxidized at 800 °C (20% in volume of $O_2$ in helium).

The powder with the finest particles class (0-50 µm) shows greatest mass gain than the as received powder, while the largest one (>100 µm) shows least mass gain. The curves of the intermediate particle-size classes (50-75 µm and 75-100 µm) fall between those extreme curves. The reproducibility of the oxidation curves of the particle-size class (75-100 µm) is the best one, so this 304L stainless steel powder fraction has been used for the kinetic study.

The first part of the mass gain curves corresponds to the heating under helium up to the introduction of oxygen at the beginning of the plateau at 800 °C. The small mass change during the first period is due to oxygen traces in helium (50 ppm).

Figure 3 illustrates the mass gain curves versus time (under isobaric and isothermal conditions) for samples oxidized at different temperatures under 20 % in volume of $O_2$. As expected, the mass gain increases with the temperature increase.

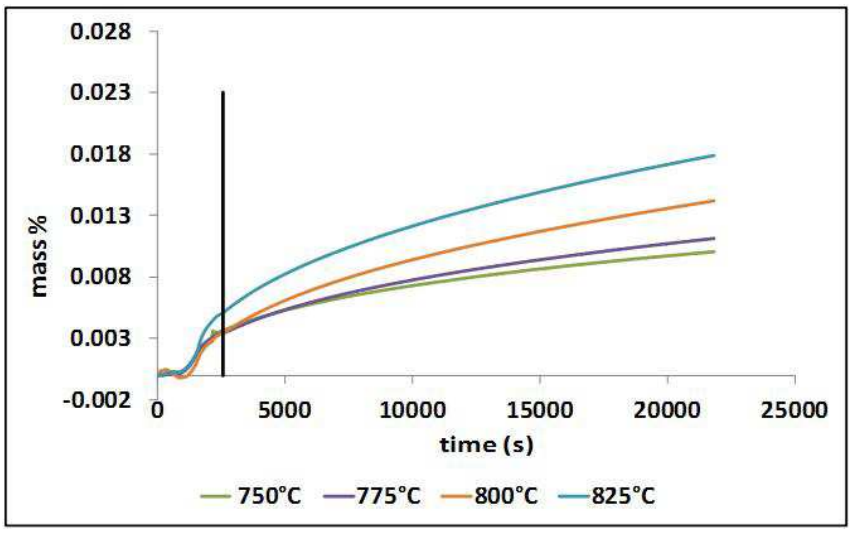


**FIGURE 3**. Mass gain (%) versus time of 75-100 µm class of 304L stainless steel powder oxidized under 20 % in volume of $O_2$ at 750 °C, 775 °C, 800 °C and 825 °C.

Figure 4 illustrates the mass gain curves versus time (under isobaric and isothermal conditions) for samples oxidized at 800 °C under 10 %, 20 % and 40 % in volume of $O_2$. The curves are superimposed; it means that there is no influence of oxygen partial pressure on the kinetic behavior of 304L stainless steel powder.

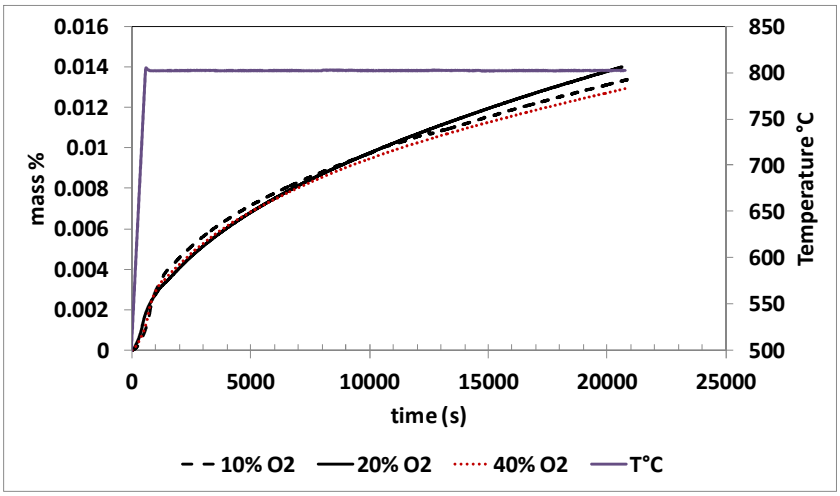


**FIGURE 4**. Mass gain (%) versus time of 75-100µm class of 304L stainless steel powder oxidized at 800 °C under 10 % (black dotted line), 20 % (black continuous line), 40 % (red fine dotted line) in volume of $O_2$.

*Characterization of 304L Stainless Steel Powder*

Figure5-a and b show individual metal alloyed particles of stainless steel powder. A native $Cr_2O_3$ layer around the particles can be observed. During water-atomization the powder is oxidized [2, 3].

a) 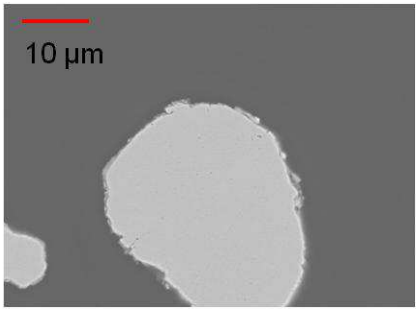


b) 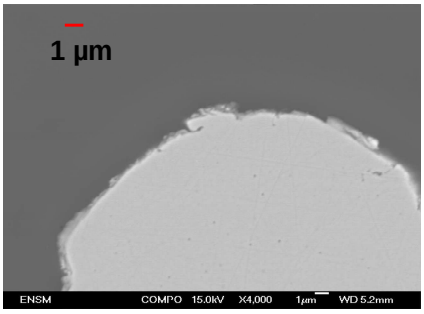


**FIGURE 5**. SEM observations of starting 304L stainless steel powder

Figures 6-a and b show SEM observations of the powder oxidized during respectively 6 hours and 20 hours. The particles exhibit an external $Cr_2O_3$ layer growth surrounding the metallic particles. The scale begins to loose adherence after 20 hours of oxidation. EDX analysis (Figure 7) shows that the outermost layer is composed of an iron rich mixed oxide phase.

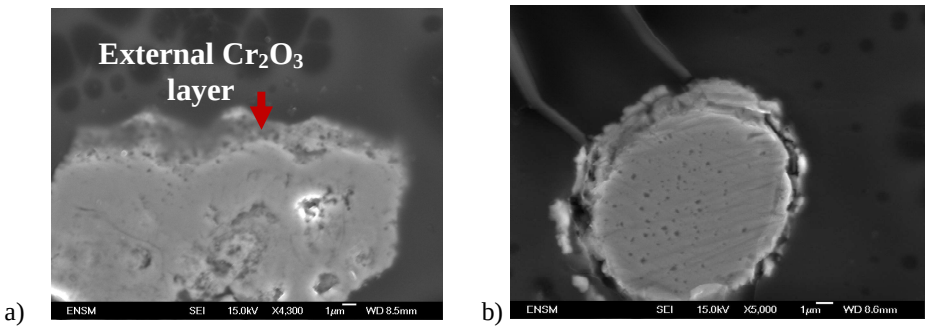


**FIGURE 6**. SEM observations of 304L stainless steel powder oxidized at 800 °C after 6 h (a) and 20 h (b)

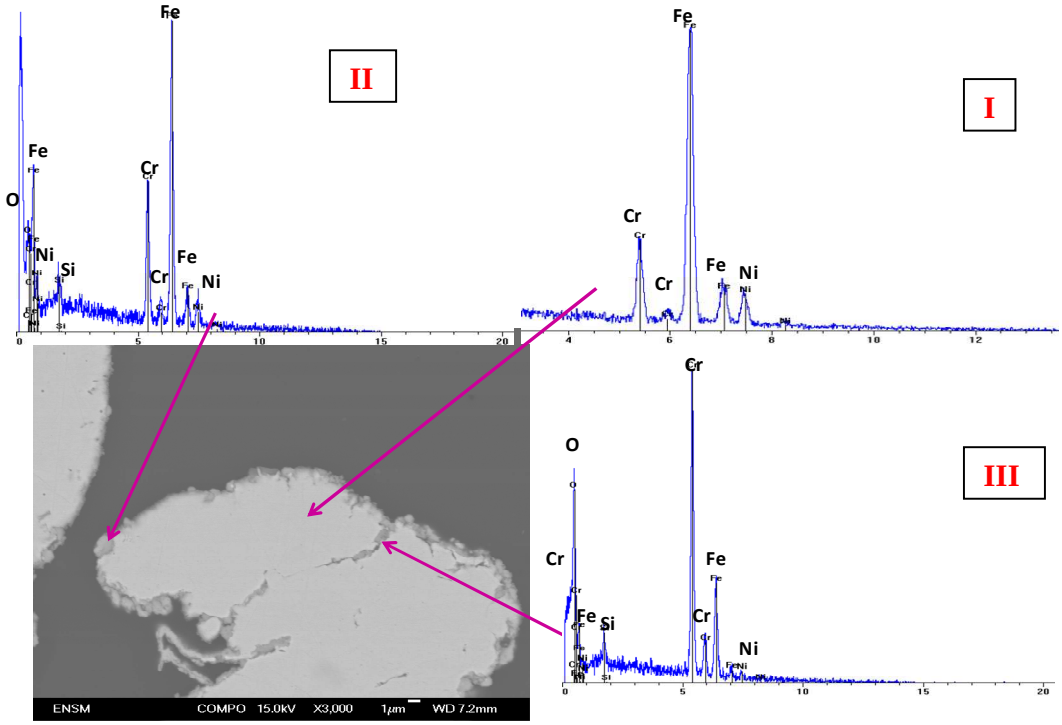


**FIGURE 7**. EDX analysis of 304L stainless steel powder oxidized at 800 °C after 20 h

## DISCUSSION

The oxidation of 304L stainless steel powder shows a parabolic like behavior with an external $Cr_2O_3$ layer growth. According to literature data concerning the oxidation of 304L foils [4, 5, 6], the oxide growth should be controlled by the diffusion of cations. Assuming that the $Cr_2O_3$ layer remains very thin compared to the particle radii, a parabolic law could account for the experimental mass gain curves. Due to the existence of an initial native oxide layer, the complete parabolic law (equation 1) has been applied to the experimental data,the mass gain is normalized by the surface area of the powder (Figure 8) [7]. The fitted value of kp is equal to $2.5 \times 10^{-12}$ $g^2$ $cm^{-4}$ $s^{-1}$ in agreement with the literature data for $Cr_2O_3$ growth (at 800°C: kp = $8 \times 10^{-12}$ $g^2.cm^{-4}.s^{-1}$) [8].

$$t = A + B\Delta m + \frac{1}{k_P}\Delta m^2 \quad (1)$$

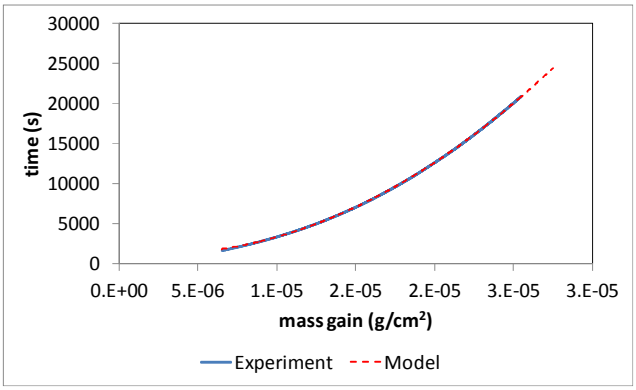


**FIGURE 8**. Oxidation of 304L stainless steel powder at 800 °C : experimental curve and complete parabolic law.

However, a much more detailed kinetic analysis can be undertaken considering the kinetics of solid-gas reactions with powders. Solid gas reaction kinetic modeling is based on the assumption of the rate determining step which can be validated using the "Φ $S_m$" test based on the jumps method [9, 10]. Such a method consists of a sudden jump in a thermodynamic variable (temperature or pressure) from an initial value to a final one and uses the ratios of the kinetic rates measured after/before this jump.

When the reaction is controlled by diffusion or by an interfacial step, the kinetic rate expressed as dα/dt (where α is the fractional conversion), is given by:

$$\frac{d\alpha}{dt} = \phi(T, Pi, \ldots).S_m(t) \quad (2)$$

where Φ (T,Pi,...) is the areic rate of growth (mol.$m^{-2}$.$s^{-1}$), and $S_m(t)$ is the space function ($m^2$.$mol^{-1}$) related to the extent of the reaction area where the rate-determining step takes place, which depends on the time and on the history of the solid. The jumps method was applied in our tests by a sudden change of the temperature from $T_0$ = 780 °C to $T_1$= 800 °C at various mass gains. Figure 9 illustrates the ratio of the kinetic rates (R) after/before the jump versus mass gain. The "Φ $S_m$" test is validated if the ratio of values does not depend of the mass gain at which the jumps are done. Figure 9 shows that we can consider two domains, in the first domain until 9 hours the ratios take a constant value around 1,45 ±0,05, in the second domain after 12 hours of treatment the ratios are also constant, the value is higher around 2 ± 0,01. The " Φ $S_m$ " test is validated in both separate domains. In each of these areas the oxidation rate of 304L powder (75-100 µm) can be decomposed into a product functions according to Equation 2. There is thus in both cases a step of the growth mechanism of the oxide which controls the speed of the reaction. However, after a certain oxidation time (from 12 hours), a different rate-determining step and / or a different mechanism should be considered. Based on the literature and SEM/EDX observations of 304L powder oxidized after 6 and 20 hours, we can assume that, at first, it is the diffusion of $Cr^{3+}$ ions which determines the rate of reaction. Then from a certain thickness of chromium oxide, it is the diffusion of $Fe^{3+}$ which limits the rate, the outer oxide layer becoming rich in iron.

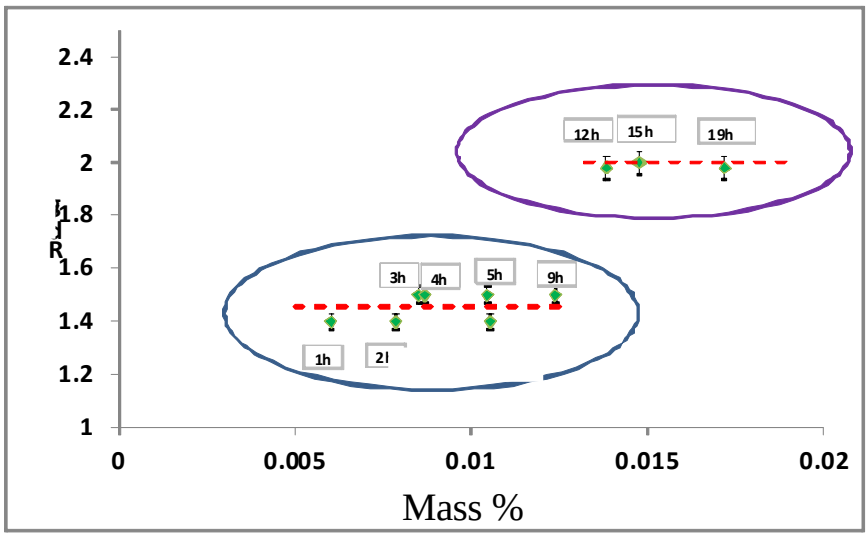


**FIGURE 9**. Oxidation of 304L stainless steel powder : ratio R for jumps changes from 780 to 800 °C (20 % $O_2$).

Assuming an Arrhenius behavior for the dependence of Φ with temperature, the activation energy calculated from the first domain ratio is about 177 kJ/mol which is rather a similar to that of $Cr/Cr_2O_3$ reaction (158 kJ/mol) [11]. For the second domain, the apparent activation energy is about 322 kJ/mol. Consequently this higher apparent activation energy should correspond to the growth of the mixed oxide rich in iron.

Kinetic model:

In the first domain (short oxidation time), the rate law can be obtained using the assumption that the rate-determining step corresponds to the external $Cr_2O_3$ oxide layer growth around the stainless steel powder particles, considered as spherical (Figure 10). The oxidation is controlled by the diffusion of Cr cations through the oxide layer.

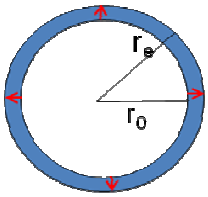


**FIGURE 10.** Scheme illustrating the oxide layer (thickness equal to $r_e$ - $r_0$) around a spherical stainless steel powder particle with a $r_0$ initial radius

The rate law is given by:

$$\frac{d\alpha}{dt} = J_{Cr} \cdot \frac{s}{n_0} \quad (3)$$

where s is the initial surface of a stainless steel particle, $n_0$ is the initial mole number of Cr in the 304L stainless steel and $J_{Cr}$, the diffusion flow in $mol.m^{-2}.s^{-1}$, is given by:

$$J_{Cr} = D_{Cr}|\Delta C| \frac{r_e}{r_0(r_e - r_0)} \quad (4)$$

where $D_{Cr}$ is the diffusion coefficient of Cr in $m^2.s^{-1}$, $\Delta C$ is the difference in the Cr concentration at both sides of the diffusion layer.

Knowing that the fractional conversion α represents the ratio between the experimental mass obtained from TGA and the theoretic mass necessary for total oxidation of chromium in the stainless steel (18 wt. %), α the fractional conversion can be written by:

$$\alpha = \frac{n_{Cr_2O_3}}{\frac{1}{2}n_0} = \frac{2}{n_0.V_{mox}}.\left(\frac{4}{3}.\pi.r_e^3 - \frac{4}{3}.\pi.r_0^3\right) \quad (5)$$

where $n_0$ is the mole number of Cr in the sample of powder of mass $m_0$

$$n_0 = \frac{m_0 . 0{,}18}{M_{Cr}} \quad (6)$$

and $n_{Cr2O3}$ is the mole number of $Cr_2O_3$ formed, $V_{mox}$ is the molar volume of $Cr_2O_3$. From equation (5), $r_e$ can be expressed by:

$$r_e = r_0 \left(1 + \frac{3.n_0.V_{mox}.\alpha}{8.\pi.r_0^3}\right)^{1/3} \quad (7)$$

with $r_0$ the mean radius equal to 43 microns considering the T-304L stainless steel powder (75-100µm) particles as spherical.

Thus the rate law can be written as:

$$\frac{d\alpha}{dt} = \phi.\frac{4.\pi.r_0}{n_0} \frac{\left(1+\frac{3.n_0.V_{mox}.\alpha}{8.\pi.r_0^3}\right)^{1/3}}{\left[\left(1+\frac{3.n_0.V_{mox}.\alpha}{8.\pi.r_0^3}\right)^{1/3} - 1\right]} \quad (8)$$

In this expression, α the fractional conversion is ratio of the experimental mass change Δm relative to the mass variation theoretically needed to oxidize the chromium in the alloy. The value of α can be calculated from the experimental mass change Δm versus time according to equation 9:

$$\alpha = \frac{\Delta m}{\Delta m_{th}} = \frac{\Delta m}{\frac{3}{4}.M_{O_2}.n_0} \quad (9)$$

with $M_{O2}$ the oxygen molecular weight.

Figure 11 represents the fits between the kinetic data (dα/dt) and the theoretical rate law considering $S_m$ function (cf. equation 2 and 8).

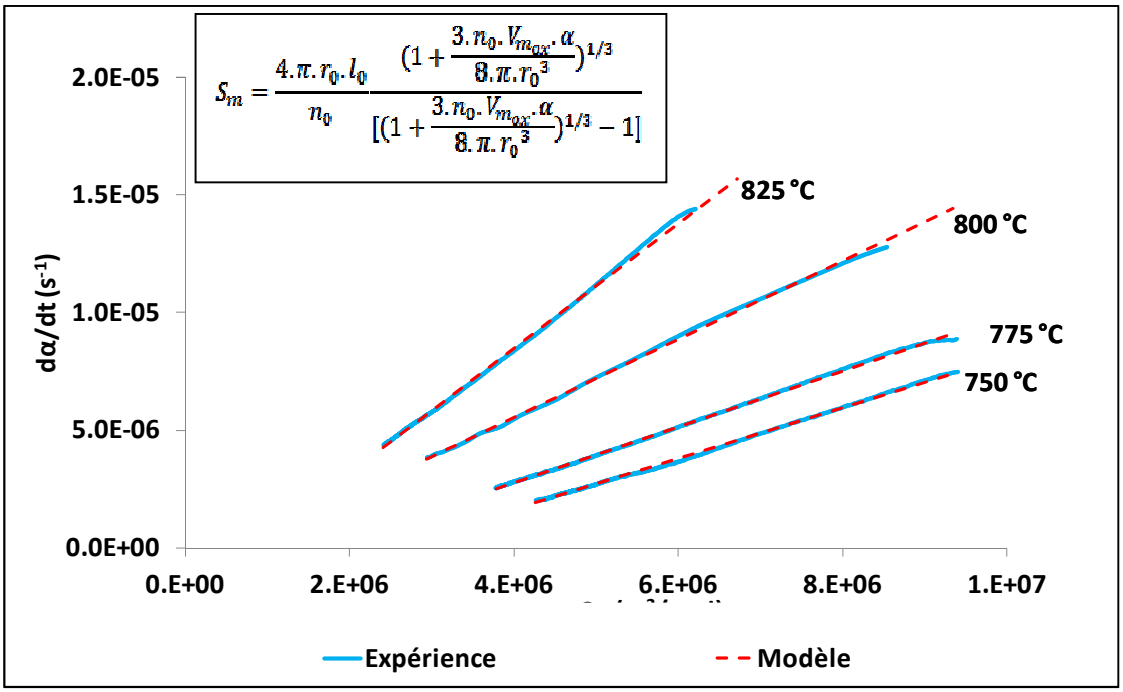


**FIGURE 11**. Oxidation of 304L stainless steel powder : experimental data (dotted curves) and theoretical rate laws (solid curves).

Only the kinetic data corresponding to the first oxidation domain between 0 and 9 hours give a straight line whose the slope of $d\alpha/dt = \Phi S_m$ give the value of $\Phi$ at each temperature. The model is thus found in good agreement with experimental data.

Table 2 shows the values of $\Phi$ for temperatures between 750 and 825 ° C.

**TABLE 2. $\Phi$ values at different temperatures**

| Temperature (°C) | $\Phi$ (mol.m$^2$.s$^{-1}$) x10$^{-12}$ |
|---|---|
| 750 | 0,76 |
| 775 | 0,85 |
| 800 | 1,59 |
| 825 | 2,13 |

Based on these data, and plotting ln $\Phi$ as a function of 1/T (Figure 12), a straight line is obtained with an acceptable coefficient of correlation showing that $\Phi$ depends on the temperature according to the Arrhenius law. The apparent activation energy obtained is equal to 139 kJ / mol. This value is significantly lower than that of the value previously calculated from the ratio of the kinetic rates in the short time period (cf. Figure 9), but nevertheless, the two methods of calculation give values of apparent activation energy close to 158 kJ / mol, which correspond to the system $Cr/Cr_2O_3$.

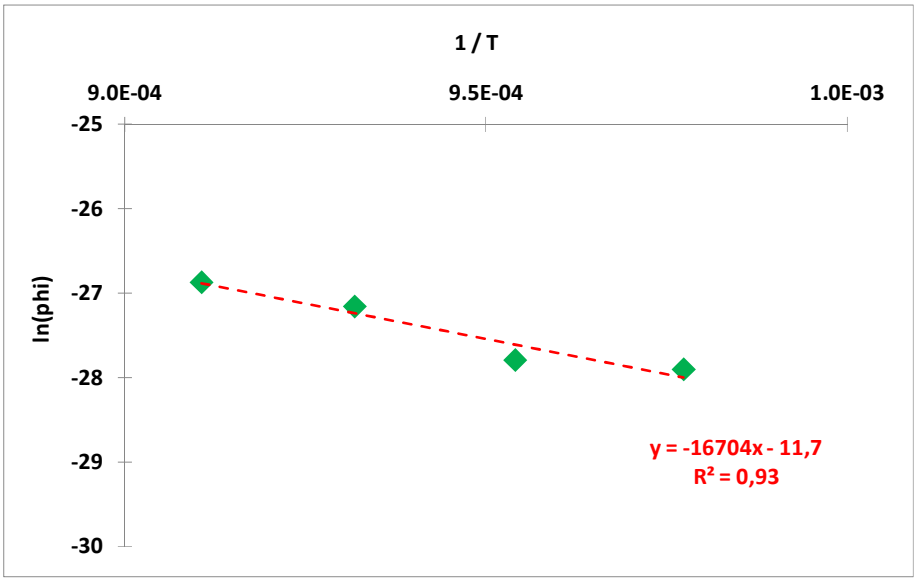


**FIGURE 12.** Variation of ln Φ versus 1 / T ($K^{-1}$)

Relation between Φ and $k_p$

Φ et $k_p$ are temperature dependent and they represent quantities obtained for the same diffusion controlling step but in different geometries (spheres and plates respectively). In a planar geometry, the fractional conversion α is given by:

$$\alpha = \frac{4}{3}.\frac{1}{n_0 M_{O_2}}.\Delta m \quad (10)$$

The kinetic rate is given by:

$$\frac{d\alpha}{dt} = \phi.S_m = \phi.\frac{l_0}{X}.\frac{s}{n_0} \quad (11)$$

where $l_0$ is a lenght equal to unity (1m), X is the thickness of the oxide layer expressed by Equation 12:

$$X = \frac{2Vm_{ox}}{3M_{O_2}}.\frac{\Delta m}{s} \quad (12)$$

The relationship between $k_p$ and Φ is established from the combination of Equation 11 and of the derivative of Equation 1,

$$k_p = \frac{l_0 3^2 M_{O_2}{}^2}{4Vm_{ox}}\phi \quad (13)$$

At 800 °C, based on the value of Φ, $k_p$ is equal to $2x10^{-12}$ $g^2.cm^{-4}.s^{-1}$. This value is in good agreement with the value found using the complete parabolic law: $k_p = 2.5x10^{-12}$ $g^2.cm^{-4}.s^{-1}$ and with literature data confirming the similar behavior between 304L plates and powder.

## CONCLUSION

This study has put in evidence a conventional oxidation of the 304L stainless steel powder with a parabolic like behavior. The fitted $k_p$ value calculated with a complete parabolic law or with $\Phi$ the areic rate of growth is similar to literature data. A $Cr_2O_3$ external layer has been observed after short time oxidation test. When the oxidation time is increase a mixed iron rich external scale is also observed. The diffusion of cations is the rate determining step of the external oxide layer growing. A detailed modeling kinetic analysis has been done based on the jumps methods. The rate law has been writen considering spherical stainless steel powder particle. The model is in good agreement with the experimental data. We can therefore conclude that the 304L powder has the same behavior than alloy plates of the same composition.

This study will help us to understand the unusual oxidation behavior of a model composite elaborated with 304L stainless steel particles inserted in an yttrium stabilized zirconia matrix which seems to play a basic role in the early stage of the composite oxidation process.

## REFERENCES


1. M. Nanko, Science and Technology of Advanced Materials, 6, (2005), pp.129-134.
2. A. Nylund, T. Tunberg, H. Bertilsson, E. Carlstrom, I. Olefjord, The international journal of powder metallurgy, 31 (1995), pp.365-373.
3. M. Norell, A. Nyborg, T. Tunberg, I. Olefjord, Surface and interface analysis, 19 (1992), pp.71-76.
4. V. Alenka, M. Mozetic, A. Zalar, Applied Surface Science, 200, (2002), pp. 94-103.
5. H. Asteman, J.E. Svensson, L.G. Johansson, Oxidation of Metals, 57, (2002), pp. 193-216
6. F. Riffard, H. Buscail, E. Caudron, R. Cueff, C. Issartel, S. ElMesski and S. Perrier Materials, Science Forum, 461-464,(2004), pp.175-182
7. D. Monceau and B. Pieraggi, Oxidation of Metals, 50, (1998), pp.477-493.
8. P. Kofstad, High- temperature Corrosion (1988).
9. M. Pijolat and M. Soustelle, Thermochimica Acta 478, (2008), pp. 34-40.
10. K. Surla, F. Valdivieso, M. Pijolat, M. Soustelle, M. Prin, Solid State Ionics 143, (2001), pp. 355-365
11. D.Young, High Temperature Oxidation and Corrosion of Metals, Elsevier Corrosion Series (2008).